

# A Fast Multipole Method for axisymmetric domains

Michael J. Carley

January 4, 2023

## Abstract

The Fast Multipole Method (FMM) for the Poisson equation is extended to the case of non-axisymmetric problems in an axisymmetric domain, described by cylindrical coordinates. The method is based on a Fourier decomposition of the source into a modal expansion and the evaluation of the corresponding modes of the field using a two-dimensional tree decomposition in the radial and axial coordinate. The field coefficients are evaluated using a modal Green's function which can be evaluated using well-known recursions for the Legendre function of the second kind, and whose derivatives can be found recursively using the Laplace equation in cylindrical coordinates. The principal difference between the cylindrical and Cartesian problems is the lack of translation invariance in the evaluation of local interactions, leading to an increase in computational effort for the axisymmetric domain. Results are presented for solution accuracy and convergence and for computation time compared to direct evaluation. The method is found to converge well, with ten digit accuracy being achieved for the test cases presented. Computation time is controlled by the balance between initialization and the evaluation of local interactions between source and field points, and is about two orders of magnitude less than that required for direct evaluation, depending on expansion order.

## 1 Introduction

Since its development [8], the Fast Multipole Method (FMM) has become the algorithm of choice for a large class of problems which can be expressed in terms of finding at a large number of field points the potential generated by a large number of point sources. This includes problems governed by the Poisson and Helmholtz equations, including boundary integral problems in acoustics, electromagnetism, and fluid dynamics, and volume integrals such as the Biot-Savart

integration which arises in electromagnetism and vortex dynamics. The method is now highly developed with efficient implementations available in two [4] and three [10] dimensions for a range of problems, using a variety of analytical tools for their formulation.

Despite its power and importance, the FMM does not seem to have been extended to non-Cartesian coordinate systems. In particular, there do not seem to be formulations of the method which can be applied to axisymmetric domains described using cylindrical coordinates. These systems arise naturally in a range of applications and cylindrical coordinates are a natural way to describe a system, or to apply boundary conditions. The purpose of this paper is to present an extension of the FMM for the Poisson equation to cylindrical coordinates, motivated by applications in fluid dynamics, where boundary and volume integral problems are governed by the Laplace kernel.

To the author's knowledge, there have been two previous studies which are relevant to this problem. The first was the work of Strickland and Amos [11, 12] who developed an accelerated method for the evaluation of the axisymmetric stream function in vortex dynamics, equivalent to solving the Poisson problem or evaluating the Biot-Savart integral. The authors used single-precision arithmetic and a fifth order expansion of the Green's function to achieve five-digit accuracy at a cost of 1–3% of the computational effort required for direct evaluation of the potential and velocity fields. The authors do not seem to have extended their method to the general case in a cylindrical domain.

More recently, in an unpublished thesis, Churchill [2] considered the general non-axisymmetric problem, motivated by the analysis of boundary integrals on surfaces of revolution. He identifies the particular difficulty in cylindrical coordinates, which is that the Green's function is translation invariant in the axial coordinate, but not in the radial, which complicates the evaluation of interactions which arise in the FMM. He concludes that the problem can be solved using a black-box [5] or generalized [6] FMM, but does not present results for the cylindrical problem.

This paper presents a method for the fast evaluation of the potential in a cylindrical domain, generated by a set of azimuthally varying ring sources. The motivation is the Poisson or Biot-Savart problem in fluid dynamics, with the expectation that the method is to be used in boundary integral solvers [13, for example], or in evaluating the velocity field due to a distribution of vorticity [12]. The approach is essentially that of a standard two-dimensional FMM, with modifications to the evaluation of interactions to accommodate the lack of translation invariance. It is assumed that any necessary Fourier transformation of the inputs to the calculation has been performed, so that the starting point is the location and radius of a set of circular sources, and the coefficients of the Fourier series for a source distribution on each circle. The main elements of the method are described briefly, with a

more detailed description of those parts which are particular to the axisymmetric case, i.e. the evaluation of the Green's function and its derivatives in cylindrical coordinates. Results are presented for a problem with an increasing number of sources, to test the performance of the method for convergence and speed.

## 2 Analysis

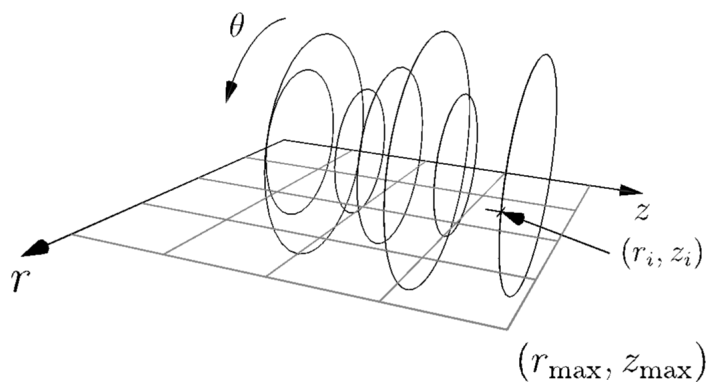


Figure 1: Basic problem: ring sources of radius  $r_i$  are distributed at axial station  $z_i$  in the domain  $0 \leq r \leq r_{\max}$ ,  $0 \leq z \leq z_{\max}$ . Sources are given as the coefficients of the Fourier series of source strength as a function of  $\theta$  at each  $(r_i, z_i)$

The problem to be solved is sketched in Figure 1. We assume that any necessary preprocessing has been performed to reduce the system to the form shown here. A set of ring sources with a common axis are distributed throughout the domain  $(r, z)$ . The source strength  $s(\theta_1)$  on a ring at location  $(r_1, z_1)$  is given by the Fourier series,

$$s(\theta_1) = \sum_{n=-N}^N S^{(n)} e^{in\theta_1}, \quad (1)$$

where subscript 1 denotes source coordinates. The potential  $\phi(r, z)$  due to the source is given by integration over  $\theta_1$ ,

$$\phi(r, \theta, z) = \int_0^{2\pi} \frac{s(\theta_1)}{4\pi R} d\theta_1, \quad (2)$$

$$R^2 = r^2 + r_i^2 - 2rr_i \cos(\theta - \theta_1) + (z - z_1)^2.$$

Under an elementary transformation, and substituting the Fourier series for  $s(\theta_1)$ ,

$$\phi(r, \theta, z) = \sum_{n=-N}^N S^{(n)} e^{-in\theta} \int_0^{2\pi} \frac{e^{in\theta_1}}{4\pi R} d\theta_1, \quad (3)$$

$$R^2 = r^2 + r_1^2 - 2rr_1 \cos \theta_1 + (z - z_1)^2.$$

The potential field  $\phi(r, z)$  can then be expressed as a Fourier series in  $\theta$ ,

$$\phi(r, \theta, z) = \sum_{n=-N}^N \Phi^{(n)}(r, z) e^{in\theta}, \quad (4)$$

$$\Phi^{(n)} = S^{(n)} G^{(n)}(r, r_1, z - z_1), \quad (5)$$

$$G^{(n)}(r, r_1, x) = \int_0^{2\pi} \frac{e^{in\theta_1}}{4\pi R} d\theta_1 = \int_0^{2\pi} \frac{\cos n\theta_1}{4\pi R} d\theta_1, \quad (6)$$

$$R^2 = r^2 + r_1^2 - 2rr_1 \cos \theta_1 + x^2.$$

The source term  $s(\theta_1)$  is assumed real, so that the complex Fourier coefficients are related by  $S^{(-n)} = (S^{(n)})^*$ . Henceforth, all computations will be performed for  $n \geq 0$  and the conjugate relationship will be assumed.

We refer to  $G^{(n)}(r, r_1, x)$  as the *modal Green's function* relating Fourier coefficients of the source to those of the potential at some other point. Appendix A gives details of the evaluation of  $G^{(n)}(r, r_1, x)$  and of its derivatives. In particular, it is shown that it can be expressed exactly as

$$G^{(n)}(r, r_1, x) = \frac{Q_{n-1/2}(\chi)}{2\pi\sqrt{rr_1}}, \quad (7)$$

where  $Q_\nu(\chi)$  is a Legendre function of the second kind [3].

Given a distribution of sources at locations  $(r_i, z_i)$ ,  $i = 1, \dots, N_s$ , each of which has a set of Fourier coefficients  $S_i^{(n)}$ ,  $n = 0, \dots, N$ , the problem to be solved is then the approximate evaluation of the sum

$$\Phi^{(n)}(r_j, z_j) = \sum_{i=1}^{N_s} S_i^{(n)} G^{(n)}(r_j, r_i, z_j - z_i), \quad (8)$$

for field points  $(r_j, z_j)$ ,  $j = 1, \dots, N_f$ .

## 2.1 Outline of the FMM

The Fast Multipole Method is well established and there are numerous guides to its algorithm and implementation. Here we give an outline of the method in order

to present the necessary terminology and to indicate those parts of the algorithm of this paper which differ from existing methods. From the previous section, we recall that the objective is to approximately evaluate the sum

$$\Phi^{(n)}(r_j, z_j) = \sum_{i=1}^{N_s} S_i^{(n)} G^{(n)}(r_j, r_i, z_j - z_i), \quad n = 0, \dots, N, \quad j = 1, \dots, N_f,$$

given a list of source and field points  $(r_i, z_i)$  and  $(r_j, z_j)$  respectively. The first operation of the FMM is the sorting of points and their representation in a quadtree data structure, formed by repeated subdivision of the domain  $0 \leq r_{i,j} \leq r_{\max}$ ,  $0 \leq z_{i,j} \leq z_{\max}$ ,  $z_{\max} = r_{\max}$ . Figure 2 shows the repeated halving of intervals. At each *level* of subdivision  $\ell$ , the domain is divided into  $2^\ell \times 2^\ell$  boxes, to a maximum level called the *depth* of the tree  $d$ . Boxes in the tree can be indexed by their location  $(i, j)$  on the grid at a given level, or by their Morton index.

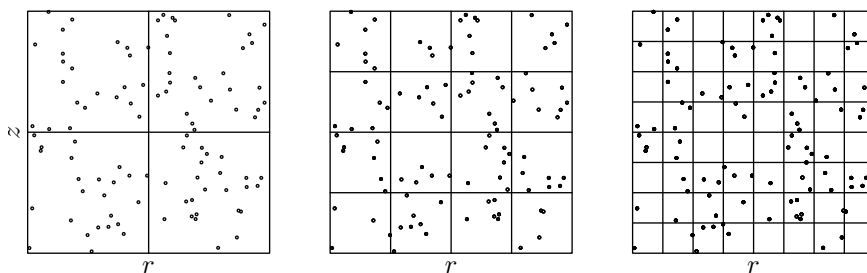


Figure 2: Recursive subdivision of the source domain into  $4^\ell$  boxes for  $\ell = 1, 2, 3$ , left to right

Figure 3 gives the terminology for relationships between boxes. A box at grid location  $(i, j)$  at level  $\ell$  has four *child* boxes at grid locations  $(2i, 2j)$ ,  $(2i, 2j + 1)$ ,  $(2i + 1, 2j)$ ,  $(2i + 1, 2j + 1)$  at level  $\ell + 1$ , and has a *parent* box at grid location  $(i/2, j/2)$  at level  $\ell - 1$ . A box at the finest level of subdivision, depth  $d$ , has no children and is called a *leaf* box.

*Neighbors* of box  $(i, j)$  are boxes at the same level  $\ell$  which share at least a vertex with the box, including the box itself. In Figure 3, boxes 1–9 are neighbors of box 1. All other boxes are said to be in the *far field* of box 1. The basic principle of the FMM is to separate far-field from neighbor interactions and evaluate the far-field terms in any box using an accelerated summation.

This is achieved in the first instance by evaluating the field due to sources inside a box using an approximate expansion which is faster than direct evaluation of the sum

$$\Phi^{(n)}(r, z) = \sum_i S_i^{(n)} G^{(n)}(r, r_i, z - z_i),$$

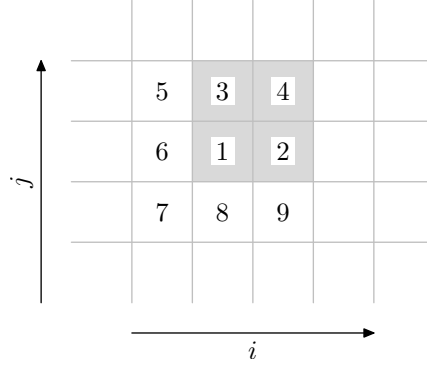


Figure 3: Terminology for relationships between boxes: boxes 1–4 are children of the shaded box; the shaded box is the parent of boxes 1–4; boxes 1–9 are neighbors of box 1

where the summation is taken over all sources inside a box. At field points sufficiently far from the box, the Green’s function for a source is well approximated by its Taylor series, truncated to some order  $M$ ,

$$G^{(n)}(r + \Delta r, r_1 + \Delta r_1, x + \Delta x) \approx \sum_{m=0}^M \sum_{i+j+k=m} \bar{g}_{i,j,k}^{(n)} (\Delta r)^i (\Delta r_1)^j (\Delta x)^k, \quad (9)$$

$$\bar{g}_{i,j,k}^{(n)} = \frac{1}{i!} \frac{1}{j!} \frac{1}{k!} \frac{\partial^{i+j+k}}{\partial r^i \partial r_1^j \partial x^k} G^{(n)}(r, r_1, x).$$

Details of the evaluation of the derivatives of  $G^{(n)}$  are given in Appendix A.

The field at a point  $(r, z)$  due to a source at  $(r_1 + \Delta r_1, z_1 + \Delta z_1)$  in a box with center  $(r_1, z_1)$  is then given by

$$\Phi^{(n)}(r, z) \approx S^{(n)} \sum_{m=0}^M \sum_{i+j=m} (-1)^j \bar{g}_{0,i,j}^{(n)} (\Delta r_1)^i (\Delta z_1)^j, \quad (10)$$

noting that  $x = z - z_1$  and  $\partial/\partial z_1 = -\partial/\partial x$ . Summing over all sources contained in the box,

$$\Phi^{(n)}(r, z) \approx \sum_{m=0}^M \sum_{i+j=m} (-1)^j \bar{g}_{0,i,j}^{(n)} S_{ij}^{(n)}, \quad (11)$$

where the moments  $S_{ij}$  are given by

$$S_{ij}^{(n)} = \sum_q S_q^{(n)} (\Delta r_q)^i (\Delta z_q)^j. \quad (12)$$

To initialize the source data in the first stage of the FMM, the moments  $S_{ij}^{(n)}$  are computed for each leaf box in the tree. In the *upward pass*, the moments at boxes in each level  $\ell$  are computed, for  $\ell = d - 1, \dots, 1$ . This can be achieved without requiring direct evaluation of moments from source data, by combining moments from child boxes to generate moments in their parent box, Figure 4. Moments about the center of a child box at displacement  $(\Delta r, \Delta z)$  contribute to the moments about the center of their parent box via

$$S_{ij} = \sum_{q=0}^i \sum_{u=0}^j \binom{i}{q} \binom{j}{u} (-\Delta r)^q (-\Delta z)^u S'_{i-q, j-u}, \quad (13)$$

where the superscript  $(n)$  has been suppressed for clarity. When the upward pass has been completed, each box at levels  $\ell = 1, \dots, d$  contain a set of moments which can be used to estimate the potential in the far field of the box.

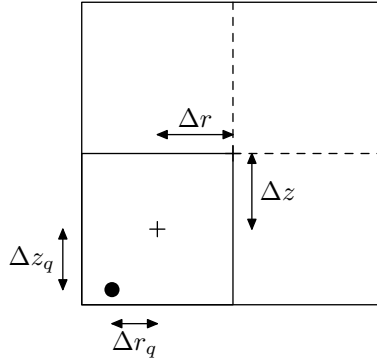


Figure 4: Evaluation and shifting of source moments: moments about the center of the leaf box are computed using (12); those about the center of the parent box are computed by shifting the child box moments by  $(\Delta r, \Delta z)$  using (13).

In the next stage of the FMM, the *downward pass*, each box is assigned a *local expansion* which can be used to evaluate the potential inside the box due to sources which lie in its far field. The core of the FMM is the use of the most efficient expansion possible at any level to evaluate the far-field terms in any box. The field in a box centered at  $(r, z)$  is given by

$$\Phi^{(n)}(r + \Delta r, z + \Delta z) = \sum_{m=0}^M \sum_{k+\ell=m} \Phi_{k\ell}^{(n)} (\Delta r)^k (\Delta z)^\ell, \quad (14)$$

where the expansion coefficients  $\Phi_{k\ell}^{(n)}$  are evaluated from the contributions of sources in boxes which interact with the field box. The order  $M$  of the local

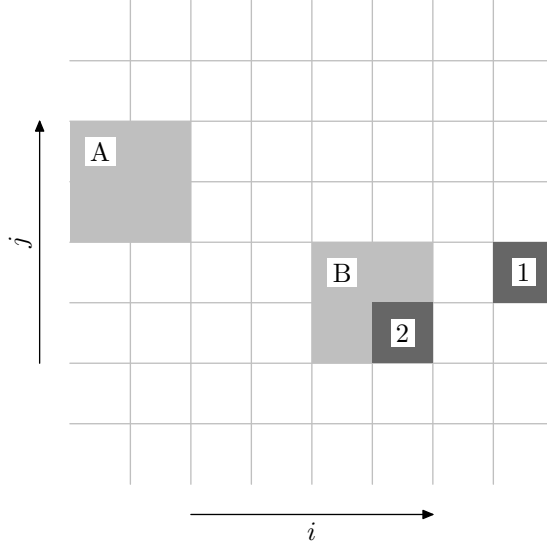


Figure 5: Generation of a local field in a box: the local expansion of the field in box B due to sources in box A is computed using the S2L operation, (15); the local expansion in box 2 is found by shifting the expansion in box B to box 2 and adding the contribution from box 1, evaluated using an S2L operation.

expansion at any level is not required to be the same as the order of the source expansions, but has been set equal for the calculations presented in this paper.

Figure 5 shows the main operations involved, for the evaluation of a local expansion in box 2, which has parent box B. On the downward pass, the local expansion in box B is found by adding the contribution from sources in boxes which are well separated from B, such as box A. This contribution is found using the *shift-to-local* or S2L operation. The local expansion in B is used to generate the local expansion in each of its child boxes, including box 2. Box 2 then has its local expansion incremented by the contribution of boxes with which it interacts, such as box 1. At the end of the downward pass, each leaf box has a local expansion which accounts for the contribution of all sources lying outside its neighbors.

The two operations to be implemented here are the S2L and the parent-to-child shift of the local expansion. The S2L shift is found by differentiating (10),

$$\Phi_{k\ell}^{(n)} = \sum_{i,j} (-1)^j \binom{j+\ell}{j} S_{ij}^{(n)} \bar{g}_{k,i,j+\ell}^{(n)}, \quad (15)$$

which can be implemented as a BLAS level 2 operation

The local expansion in a child box at displacement  $(\Delta r, \Delta z)$  is given from the



parent box expansion by,

$$\Phi_{ij} = \sum_{q=0} \sum_{u=0} \binom{i+q}{q} \binom{j+u}{u} (-\Delta r)^q (-\Delta z)^u \Phi'_{i+q,j+u}, \quad (16)$$

where terms  $\Phi'_{i,j}$  are coefficients of the parent box local expansion.

## 2.2 Evaluation of interactions

The outline of the Fast Multipole Method presented in subsection 2.1 contains the main elements of a generic FMM which are familiar from existing implementations. In this section, we describe the part of the algorithm which is particular to the cylindrical domain, the S2L operation for the modal Green's function. In existing, Cartesian, methods, the translation operators are invariant with respect to shifts in the coordinate system. As noted by Churchill [2], however, this is not true for the modal Green's function  $G^{(n)}$ , which is invariant for shifts in the axial coordinate  $z$  but not for displacements in radius  $r$ . This increases the number of orientations for which shift operators must be computed, though there are still some symmetries which can be exploited to reduce the workload.

Recall that the modal Green's function is given by

$$G^{(n)}(r, r_1, x) = \frac{Q_{n-1/2}(\chi)}{2\pi\sqrt{rr_1}}, \quad \chi = \frac{r^2 + r_1^2 + x^2}{2rr_1}, \quad x = z - z_1.$$

This is invariant under translations in  $z$  and is symmetric in  $r$  and  $r_1$ , a fact which is exploited in the recursion relations for derivatives in source and field coordinates [11, 12]. To take advantage of this symmetry, we introduce some terminology to describe translation operations. If we assume that for S2L operations, we evaluate derivatives of  $G^{(n)}(r, r_1, x)$  for the  $r \geq r_1, x \geq 0$ . Then, from Figure 6, we can derive translation operators for four different cases. These correspond to shifts in the positive or negative (forward or backward) axial direction, and from greater to smaller radius (outward or inward).

The basic operator, which uses the derivatives of the Green's function without modification, is the *forward-outward* or FO shift, (15).

$$\Phi_{k\ell}^{(n)} = \sum_{i,j} (-1)^j \binom{j+\ell}{j} S_{ij}^{(n)} \bar{g}_{k,i,j+\ell}^{(n)}.$$

For the *backward-outward* or BO shift,  $x < 0$ ,  $\partial/\partial z_1 = \partial/\partial x$  and  $\partial/\partial z = -\partial/\partial x$ , yielding

$$\Phi_{k\ell}^{(n)} = \sum_{i,j} (-1)^\ell \binom{j+\ell}{j} S_{ij}^{(n)} \bar{g}_{k,i,j+\ell}^{(n)}.$$

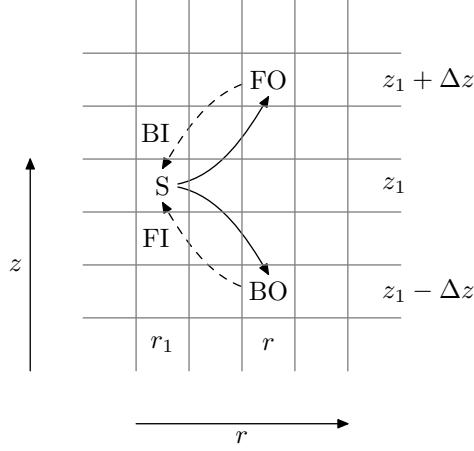


Figure 6: Reuse of Green's function derivatives for forward/backward and inward/outward interactions. The source box  $S$  generates local expansions at  $r > r_1$  through a forward-outward (FO) and a backward-outward (BO) operation, indicated by solid arrows. The boxes at greater radius generate local expansions in box  $S$  via backward-inward (BI) and forward-inward (FI) operations. All four operations are computed from the same expansion of the Green's function.

To evaluate the inward shifts, we exchange  $r$  and  $r_1$  and swap the corresponding indices. For the *forward-inward* S2L operation,

$$\Phi_{k\ell}^{(n)} = \sum_{i,j} (-1)^j \binom{j+\ell}{j} S_{ij}^{(n)} \bar{g}_{i,k,j+\ell}^{(n)},$$

which gives the contribution of the sources in the box at larger radius  $r$  to the local expansion in the box at smaller radius  $r_1$ . Finally, the *backward-inward* operator is given by

$$\Phi_{k\ell}^{(n)} = \sum_{i,j} (-1)^\ell \binom{j+\ell}{j} S_{ij}^{(n)} \bar{g}_{i,k,j+\ell}^{(n)}.$$

In order to apply the shift operations, we enumerate candidate source boxes which may contribute to the field in a box, Figure 7. This gives rise to two interaction lists, the D list containing boxes which contribute via direct evaluation of the field for each source and field point, and the S2L list, whose contributions are evaluated using the S2L operation acting on source and local expansion coefficients. Figure 7 indicates that the D list is made up of neighbors of box B, leaving 27 boxes which may contribute to the field in B via S2L operations. Contributions from all other boxes are transferred into B from its parent box during the downward pass. Using the axial translation invariance and the symmetry in  $r$

	S2L	S2L	S2L	S2L	S2L	S2L	
	S2L	S2L	S2L	S2L	S2L	S2L	
	S2L	D	D	D	S2L	S2L	
	S2L	D	B	D	S2L	S2L	
	S2L	D	D	D	S2L	S2L	
	S2L	S2L	S2L	S2L	S2L	S2L	

Figure 7: Interaction lists for box B. Parent box of B is shown shaded; boxes marked D have interactions evaluated directly from (8); boxes marked S2L have interactions evaluated via source-to-local operation. Unmarked boxes interact with B through its parent box so that the interactions need not be explicitly evaluated.

and  $r_1$  reduces the number of Green's function expansions to evaluated to twelve, those for boxes at  $z \geq z_1$  and  $r \geq r_1$ . The expansions are identical for any value of  $z - z_1$  but must be updated for each  $r_1$  during the downward pass. Once generated, the expansion is used to update the local expansion on the outer boxes, and to include the contribution of those boxes' source terms to the local expansion on B.

Finally, we note that the modal Green's function can be written using scaled coordinates, so that

$$G^{(n)}(\sigma r, \sigma r_1, \sigma x) = \frac{1}{\sigma} G^{(n)}(r, r_1, x), \quad (17)$$

which would allow for the shift operators to be precomputed and generated at each level as required. This has been implemented but found not to give a time saving, since each level of the tree requires twice as many shift operators as its parent level, half of which are new. In practice, we find that the bottleneck in the code is the evaluation of direct interactions rather than the computation of the S2L operators.

### 3 Algorithm

Combining the elements of the previous sections, we present an algorithm for a uniform Fast Multipole Method in an axisymmetric domain. Input is a list of  $N_s$  source points  $(r_i, z_i)$ ,  $i = 1, \dots, N_s$  and modal amplitudes  $S_i^{(n)}$ ,  $n = 0, \dots, N$ , and a list of  $N_f$  field points  $(r_j, z_j)$ ,  $j = 1, \dots, N_f$ .

---

**Algorithm 1** Fast Multipole Method for cylindrical coordinate systems

---

```

set tree depth  $d$ 
sort source points  $(r_i, z_i)$  and field points  $(r_j, z_j)$  by Morton index and assign
to leaf nodes at level  $d$ 
calculate leaf box moments from source amplitudes (12)
{upward pass}
for  $\ell = d - 1, \dots, 2$  do
    evaluate box moments at level  $\ell$  from child box moments at level  $\ell + 1$ , (13)
end for
{downward pass}
for  $\ell = 2, \dots, d$  do
    for  $i = 0, \dots, 4^{\ell-1} - 1$  do
        shift parent box local expansion from level  $\ell - 1$  to level  $\ell$  boxes
    end for
    for  $i = 0, \dots, 2^\ell - 1$  do
        evaluate coefficients of Green's function expansions for radial station  $i$ 
        for  $j = 0, \dots, 2^\ell - 1$  do
            apply S2L operators for FO and BO translations of source in box  $(i, j)$ 
            apply S2L operators for FI and BI translation to update local expansion
            in box  $(i, j)$ 
        end for
    end for
end for
for  $i = 0, \dots, 4^d - 1$  do
    for field points in box  $i$  evaluate sum of local expansion and direct contribu-
    tion from neighbor boxes
end for

```

---

The implementation in Algorithm 1 is for a uniform FMM which does not generate an adaptive decomposition when assigning points to boxes. This was decided upon to reduce the number of shift operators required in evaluating box interactions.

## 4 Results

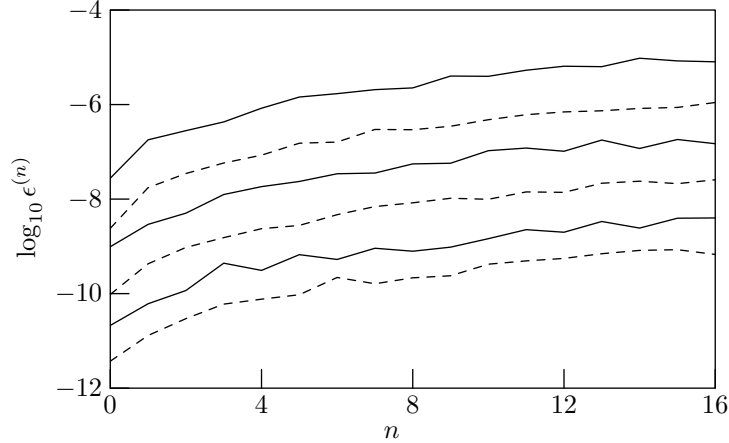


Figure 8: Error  $\epsilon$  against mode order for real part of modal amplitude  $N_s = 2^{16}$ , tree depth  $d = 6$ , expansion order  $M = 6, 8, 10, 12, 14, 16$  from top to bottom of plot.

The algorithm has been tested for accuracy and computation time using source and field points randomly distributed over  $0 \leq r, z \leq 1$ , with random modal amplitudes  $0 < S^{(n)} < 1$ ,  $n = 0, \dots, 17$ . In each case, source number  $N_s$  is set equal to number of field points  $N_f$ , with  $N_s = 2^q$ ,  $q = 10, \dots, 16$ , and the same order of expansion is used for source and field terms. Results are presented for varying  $N_s$ , maximum expansion order  $M$ , and tree depth  $d$ . Code is written in GNU C, with gcc optimization `-O3` and Goto BLAS matrix-vector operations. Calculations were performed on one core of an Intel i5-6200U laptop running at 2.3GHz. Similar code and optimizations were used for the direct evaluations used as an error reference.

Error is evaluated for each modal amplitude of the field,

$$\epsilon^{(n)} = \frac{\max |\Phi_{FMM}^{(n)} - \Phi_D^{(n)}|}{\max |\Phi_D^{(n)}|}, \quad (18)$$

where  $\Phi_{FMM}^{(n)}$  is modal amplitude evaluated using the new algorithm, and  $\Phi_D^{(n)}$  is that found by direct evaluation. Sample results for error as a function of mode number and expansion order are shown for  $N_s = 2^{16}$  in Figure 8. The method is clearly accurate, especially for higher order expansions, where eleven digit accuracy is achieved for the axisymmetric mode. The error increases at larger  $n$ , where the absolute value of the modal amplitudes is smaller, making the relative error measure larger.

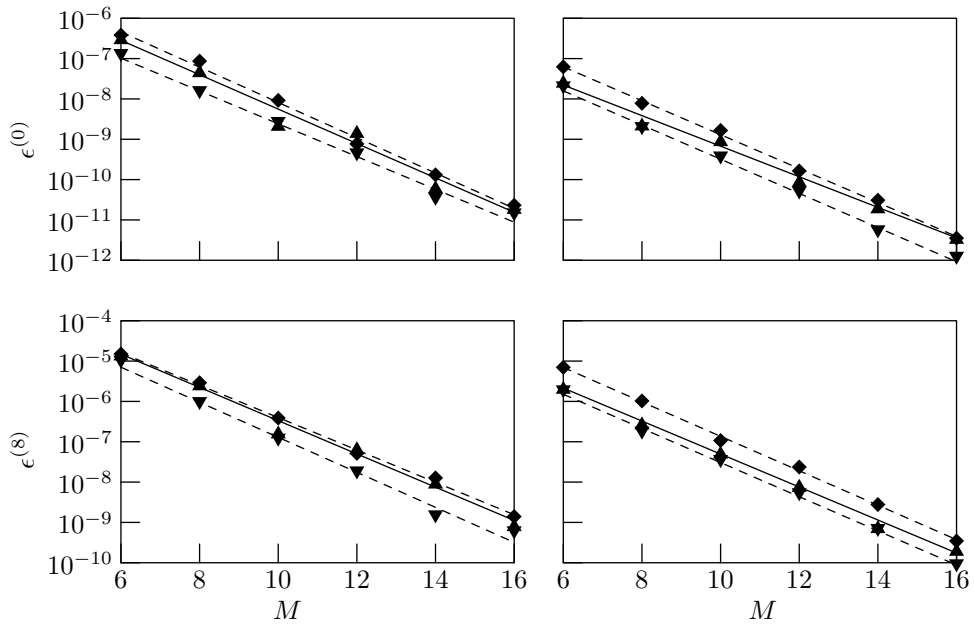


Figure 9: Error  $\epsilon$  for  $n = 0$  (top row) and  $n = 8$  (bottom row) against expansion order  $M$  for  $N_s = 2^{14}$  (left column) and  $N_s = 2^{16}$  (right column): diamonds, tree depth  $d = 5$ ; upward triangles,  $d = 6$ ; downward triangles,  $d = 7$ ; fitted lines  $\epsilon \approx C^{-0.4M}$ .

Figure 9 shows the variation in error with expansion order for the axisymmetric  $n = 0$  mode and for  $n = 8$ . The error scales approximately as  $C^{-0.4M}$  with weak dependence on tree depth. The algorithm performs well with respect to convergence over the range of problem sizes tested here.

Figure 10 shows basic data for computation time as a function of problem size. The time for direct evaluation is shown and scales at the expected  $N_f N_s = N_s^2$  rate. The computation time for the FMM algorithm behaves similarly for the low  $M = 6$  order and high  $M = 16$  order cases, with times being shifted up by the change in expansion order. The computation time in each case is roughly constant for small  $N_s$ , where the evaluation time is dominated by the set up cost, which depends on the tree depth. As the problem size increases, the evaluation time for the downward pass begins to dominate the calculation time which increases proportional to  $N_s^2$ , but with a much smaller leading constant than for direct evaluation. Again, this is the expected behavior as the direct evaluation of near-field interactions becomes the largest part of the calculation. With increasing tree depth, the box to box evaluations become correspondingly faster as the number of sources per box becomes smaller.

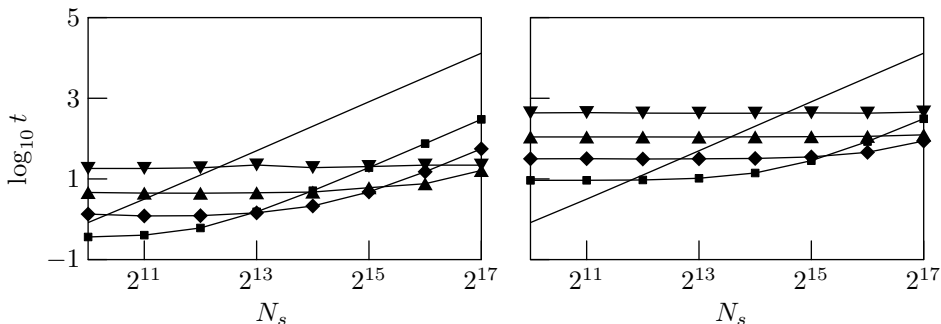


Figure 10: Computation time against source and field point number, for direct evaluation (solid line), and trees of depth 4 (boxes) depth 5 (diamonds), 6 (upward triangles), and 7 (downward triangles); left hand plot: expansion order  $M = 6$ ; right hand plot order expansion order  $M = 16$ .

Figure 11 shows the breakdown of computation time between the two parts of the calculation, as a function of tree depth. The initialization phase, made up of the upward and downward passes, scales approximately linearly with problem size, with a leading constant determined by the tree depth. Initialization time increases with tree depth, as the number of boxes increases. The time for local field evaluation, in the lower plot, scales well on  $N_s/4^d$ , the average number of sources per box, with the time reducing with tree depth. The implication is that computation time and accuracy are determined by the balance between initialization and local field evaluation, which depends on source number, expansion order, and tree

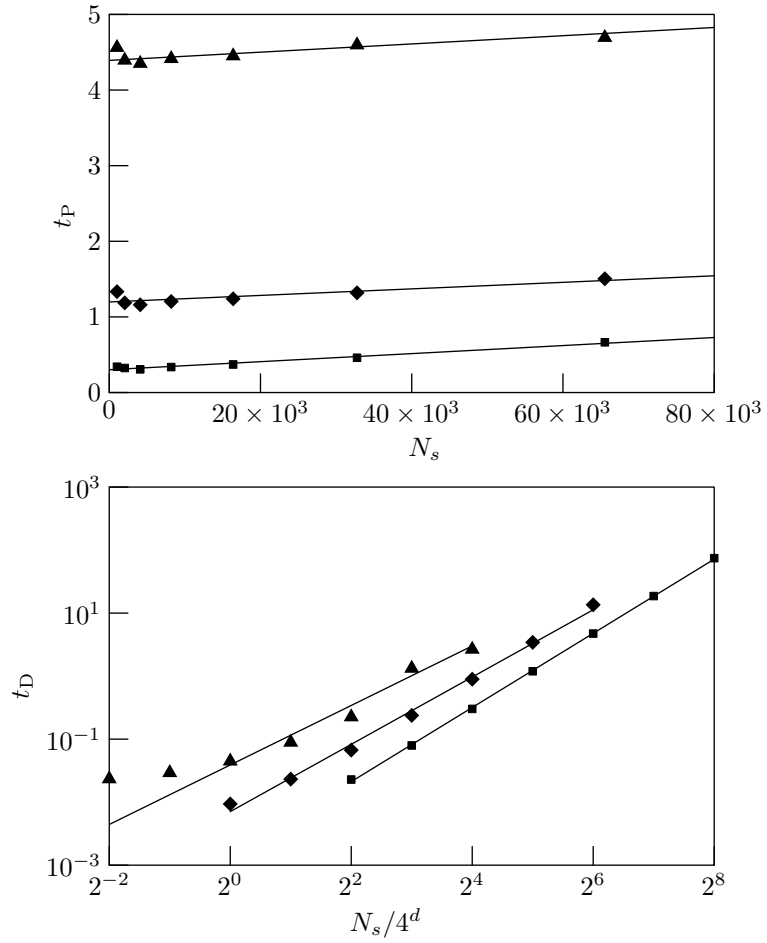


Figure 11: Execution time for phases of calculation, expansion order  $M = 6$ ; boxes: tree depth  $d = 4$ ; diamonds,  $d = 5$ , triangles,  $d = 6$ . Upper plot, time for upward and downward passes, with linear fit; lower plot, time for local field evaluation, power law fit to points with  $N_s/4^d \geq 1$ .



depth.

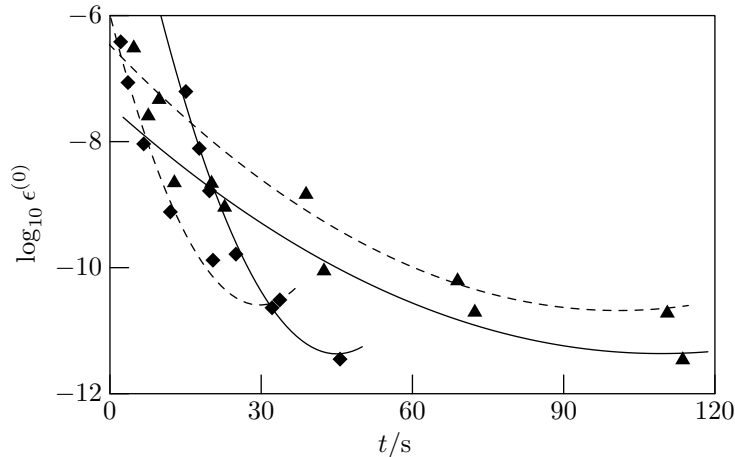


Figure 12: Error  $\epsilon^{(0)}$  against computation time: diamonds depth  $d = 5$ , triangles  $d = 6$ ; solid lines,  $N_s = 2^{16}$ ; dashed lines,  $N_s = 2^{14}$ ; curves are second order fits to  $\log \epsilon$ .

Figure 12 gives results illustrating this balance, plotting error against computation time, found by varying problem size and expansion order at two tree depths. For each tree depth and source number, there is a trend towards a minimum error, with the greater tree depth requiring a greater total computation time for higher order accuracy.

## 5 Conclusions

The Fast Multipole Method has been extended to non-axisymmetric problems in cylindrical domains, by evaluating the amplitudes of the modes in a Fourier expansion of the source and field in a Poisson problem. Testing by comparison with direct evaluation shows convergence to up to ten digit accuracy, and orders of magnitude speed-up, depending on expansion order. Open questions remain. The first is the efficient evaluation of the Legendre functions used to find the modal Green's function, which is common to the direct and fast methods, and constitutes the largest computational demand in the method. A second is the formulation of the method in a form which allows the use of BLAS level 3 operations, which should allow the code to be optimized further. Finally, we note that the approach taken here should be applicable to the Helmholtz problem, though with some greater difficulty in evaluating the modal Green's functions.

## A Evaluation of Green's functions and derivatives

The modal Green's function  $G^{(n)}(r, r_1, x)$  is defined:

$$G^{(n)}(r, r_1, x) = \int_0^{2\pi} \frac{e^{in\theta_1}}{4\pi R} d\theta_1, \quad (19)$$

$$R^2 = r^2 + r_1^2 - 2rr_1 \cos \theta_1 + x^2.$$

Cohl and Tohline [3] give an expansion for  $1/R$ ,

$$\frac{1}{R} = \frac{1}{\pi\sqrt{rr_1}} \sum_{m=-\infty}^{\infty} e^{im(\theta-\theta_1)} Q_{m-1/2}(\chi), \quad (20)$$

$$\chi = \frac{r^2 + r_1^2 + x^2}{2rr_1},$$

where  $Q_\nu(\chi)$  is the Legendre function of the second kind. Integration over  $\theta_1$  yields

$$G^{(n)}(r, r_1, x) = \frac{Q_{n-1/2}(\chi)}{2\pi\sqrt{rr_1}}. \quad (21)$$

Using the recursion for the Legendre function [7, 8.732.2], with the functional dependence on coordinates suppressed for clarity,

$$(2n-3)G^{(n-2)} = 4(n-1)\chi G^{(n-1)} - (2n-1)G^{(n)}. \quad (22)$$

For  $\chi > 1$ , the forward recursion is unstable and the backward recursion is stable, but computationally expensive [9]. To generate the sequence of modal Green's functions, we apply the approach of Helsing and Karlsson [9] and use the forward recursion for  $\chi < 1.008$ , beginning with the initial values [3],

$$Q_{-1/2}(\chi) = \mu K(\mu), \quad (23)$$

$$Q_{1/2}(\chi) = \chi\mu K(\mu) - (1+\chi)\mu E(\mu), \quad (24)$$

$$\mu = \sqrt{\frac{2}{1+\chi}}.$$

Here  $K(\cdot)$  and  $E(\cdot)$  are the complete elliptic integrals of the first and second kind respectively. These are computed using the method of Carlson [1].

For  $\chi \geq 1.008$ , the backward recursion is used starting with arbitrary values of  $Q_{n-1/2}(\chi)$  and  $Q_{n-3/2}(\chi)$  for  $n = N + 80$ , performing the downward recursion to  $n = 0$  and scaling the sequence using the known value of  $Q_{-1/2}(\chi)$ , (23). Values of  $G^{(n)}$  evaluated using this procedure have been checked against numerical integration and have been found to be correct to machine precision.

Given values of  $G^{(n)}$ ,  $n = 0, \dots, N$ , the derivatives of  $G^{(n)}$  can be found using a combination of the recursion relations for the Legendre function and the Laplace equation. For concision, we introduce the notation

$$g_{i,j,k}^{(n)} = \frac{\partial^{i+j+k}}{\partial r^i \partial r_1^j \partial x^k} G^{(n)}(r, r_1, x), \quad (25)$$

$$\bar{g}_{i,j,k}^{(n)} = \frac{1}{i!} \frac{1}{j!} \frac{1}{k!} \frac{\partial^{i+j+k}}{\partial r^i \partial r_1^j \partial x^k} G^{(n)}(r, r_1, x), \quad (26)$$

so that the Taylor series for  $G^{(n)}$  is given by

$$G^{(n)}(r + \Delta r, r_1 + \Delta r_1, x + \Delta x) = \sum_{m=0}^{\infty} \sum_{i+j+k=m} \bar{g}_{i,j,k}^{(n)} (\Delta r)^i (\Delta r_1)^j (\Delta x)^k. \quad (27)$$

The derivatives are evaluated using a recursion based on the Laplace equation, similar to the approach of Strickland and Amos who used the axisymmetric stream function equation [11, 12]. Here we use the Laplace equation for a field with azimuthal dependence  $\exp in\theta$ . This recursion requires starting values which can be found using the properties of the Legendre functions [7, 8.732]. For derivatives with respect to  $x$ ,

$$\bar{g}_{0,0,1}^{(n)} = (n - 1/2) \left[ \left( \bar{g}_{0,0,0}^{(n)} + \bar{g}_{0,0,0}^{(n-1)} \right) \frac{x}{\rho_+^2} + \left( \bar{g}_{0,0,0}^{(n)} - \bar{g}_{0,0,0}^{(n-1)} \right) \frac{x}{\rho_-^2} \right], \quad (28)$$

$$\bar{g}_{0,0,k+1}^{(n)} = (n - 1/2) \sum_{q=0}^k \frac{1}{q!(k+1)} \left[ \left( \bar{g}_{0,0,k-q}^{(n)} + \bar{g}_{0,0,k-q}^{(n-1)} \right) \frac{\partial^q}{\partial x^q} \left( \frac{x}{\rho_+^2} \right) + \right. \quad (29)$$

$$\left. \left( \bar{g}_{0,0,k-q}^{(n)} - \bar{g}_{0,0,k-q}^{(n-1)} \right) \frac{\partial^q}{\partial x^q} \left( \frac{x}{\rho_-^2} \right) \right],$$

$$\rho_{\pm}^2 = (r \pm r_1)^2 + x^2.$$

To evaluate derivatives for  $n = 0$ , the relation  $g_{i,j,k}^{(-1)} \equiv g_{i,j,k}^{(1)}$  can be used.

For the derivatives with respect to  $r$ ,

$$\bar{g}_{1,0,0}^{(n)} = -\frac{\bar{g}_{0,0,0}^{(n)}}{2r} + (n - 1/2) \frac{r^2 - r_1^2 - x^2}{2r} \left[ \left( \bar{g}_{0,0,0}^{(n)} + \bar{g}_{0,0,0}^{(n-1)} \right) \frac{1}{\rho_+^2} + \right. \quad (30)$$

$$\left. \left( \bar{g}_{0,0,0}^{(n)} - \bar{g}_{0,0,0}^{(n-1)} \right) \frac{1}{\rho_-^2} \right],$$

$$\bar{g}_{1,0,k}^{(n)} = -\frac{\bar{g}_{0,0,k}^{(n)}}{2r} + \frac{n - 1/2}{2r} \sum_{q=0}^k \frac{1}{q!} \left[ \left( \bar{g}_{0,0,k-q}^{(n)} + \bar{g}_{0,0,k-q}^{(n-1)} \right) \frac{\partial^q}{\partial x^q} \frac{r^2 - r_1^2 - x^2}{\rho_+^2} + \right. \quad (31)$$

$$\left. \left( \bar{g}_{0,0,k-q}^{(n)} - \bar{g}_{0,0,k-q}^{(n-1)} \right) \frac{\partial^q}{\partial x^q} \frac{r^2 - r_1^2 - x^2}{\rho_-^2} \right].$$

Derivatives  $g_{0,1,k}^{(n)}$  are found by exchanging  $r$  and  $r_1$ , with a corresponding swap of indices in the derivatives.

Finally,

$$\begin{aligned} \bar{g}_{1,1,k}^{(n)} = & -\frac{\bar{g}_{0,1,k}^{(n)}}{2r} \\ & + \frac{n-1/2}{2r} \sum_{q=0}^k \frac{1}{q!} \left[ \left( \bar{g}_{0,0,k-q}^{(n)} + \bar{g}_{0,0,k-q}^{(n-1)} \right) \frac{\partial^{q+1}}{\partial r_1 \partial x^q} \frac{r^2 - r_1^2 - x^2}{\rho_+^2} + \right. \\ & \left( \bar{g}_{0,1,k-q}^{(n)} + \bar{g}_{0,1,k-q}^{(n-1)} \right) \frac{\partial^q}{\partial x^q} \frac{r^2 - r_1^2 - x^2}{\rho_+^2} + \\ & \left( \bar{g}_{0,0,k-q}^{(n)} - \bar{g}_{0,0,k-q}^{(n-1)} \right) \frac{\partial^{q+1}}{\partial r_1 \partial x^q} \frac{r^2 - r_1^2 - x^2}{\rho_-^2} + \\ & \left. \left( \bar{g}_{0,1,k-q}^{(n)} - \bar{g}_{0,1,k-q}^{(n-1)} \right) \frac{\partial^q}{\partial x^q} \frac{r^2 - r_1^2 - x^2}{\rho_-^2} \right]. \end{aligned} \quad (32)$$

To compute the remaining derivatives, we make use of a recursion based on the Laplace equation in cylindrical coordinates. Noting that  $\partial/\partial\theta \rightarrow in$ ,

$$\frac{1}{r} \frac{\partial}{\partial r} \left( r \frac{\partial G^{(n)}}{\partial r} \right) - \frac{n^2}{r^2} G^{(n)} + \frac{\partial^2 G^{(n)}}{\partial x^2} = 0. \quad (33)$$

This yields the relation,

$$\bar{g}_{i+2,j,k}^{(n)} = \sum_{u=0}^i \frac{(-1)^u}{r^{u+1}} \frac{1}{(i+1)(i+2)} \left[ \frac{(u+1)n^2}{r} \bar{g}_{i-u,j,k}^{(n)} - (i-u+1) \bar{g}_{i-u+1,j,k}^{(n)} \right], \quad (34)$$

which can be used to recursively generate higher derivatives with respect to  $r$ . Switching  $r$  and  $r_1$  gives a corresponding relation for the higher derivatives with respect to  $r_1$  and allows a complete set of derivatives to be evaluated to any required order.

## References

- [1] B. C. Carlson. Numerical computation of real or complex elliptic integrals. *SIAM Journal of Numerical Analysis*, 10:13–26, 1995.
- [2] Victor Churchill. Fast multipole methods for axisymmetric geometries. M.S. Mathematics, Courant Institute of Mathematical Sciences, New York University, May 2016.

- [3] Howard S. Cohl and Joel E. Tohline. A compact cylindrical Green’s function expansion for the solution of potential problems. *The Astrophysical Journal*, 527:86–101, 1999.
- [4] Frank Ethridge and Leslie Greengard. A new fast-multipole accelerated Poisson solver in two dimensions. *SIAM Journal on Scientific Computing*, 23(3):741–760, 2001.
- [5] William Fong and Eric Darve. The black-box fast multipole method. *Journal of Computational Physics*, 228:8712–8725, 2009.
- [6] Zydrunas Gimbutas and Vladimir Rokhlin. A generalized fast multipole method for nonoscillatory kernels. *SIAM Journal on Scientific Computing*, 24(3):796–817, 2003.
- [7] I. Gradshteyn and I. M. Ryzhik. *Table of integrals, series, and products*. Academic, London, 5th edition, 1980.
- [8] L. Greengard and V. Rokhlin. A fast algorithm for particle simulations. *Journal of Computational Physics*, 73:325–348, 1987.
- [9] Johan Helsing and Anders Karlsson. An explicit kernel-split panel-based Nyström scheme for integral equations on axially symmetric surfaces. *Journal of Computational Physics*, 272:686–703, 2014.
- [10] M. Harper Langston, Leslie Greengard, and Denis Zorin. A free-space adaptive FMM-based PDE solver in three dimensions. *Communications in Applied Mathematics and Computational Science*, 6(1):79–122, 2011.
- [11] James H. Strickland and Donald E. Amos. A fast solver for systems of axisymmetric ring vortices. Technical Report SAND90-1925, Sandia National Laboratories, Albuquerque, New Mexico, 87185, United States of America, 1990.
- [12] James H. Strickland and Donald E. Amos. Fast solver for systems of axisymmetric ring vortices. *AIAA Journal*, 30(3):737–748, 1992.
- [13] P. Young, S. Hao, and P. G. Martinsson. A high-order Nyström discretization scheme for boundary integral equations defined on rotationally symmetric surfaces. *Journal of Computational Physics*, 231:4142–4159, 2012.